Leptin Receptor Positive Cells are Responsible for Fibrous Tissue Formation in Both Implant-to-Bone and Bone-to-Bone Interfaces

Vincentius J Suhardi, Anastasia Oktarina[1], Mohammed Hammad[1], Lionel B Ivashkiv[1], Mathias P G Bostrom[1], Matthew B Greenblatt[2], Xu Yang
[1]Hospital For Special Surgery, [2]Weill Cornell Medical College

INTRODUCTION:

Appropriate bone-to-bone and bone-to-implant healing is critical for the successful treatment of many orthopaedic procedures. Unfortunately, pathological fibrous healing contributes to fracture nonunions, aseptic implant loosening, failed percutaneous osseointegrated prosthesis (POP), and failed autograft-allograft interfacial healing and results in significant morbidity to patients (Nicholson, JA et al. 2021, Prock-Gibbs, H et al. 2021). Currently, treatment of these problems often requires revision surgeries which imposes additional morbidity and mortality risk (Andrzejowski, P et al. 2019, Abu-Amer, Y et al. 2007). Despite the widespread clinical prevalence of these problems, there is still a gap in knowledge of the origin of cells implicated these fibrotic processes. Here, we showed that $LepR^+$ lineage cells are abundant in the fibrous tissue in the fracture nonunion and peri-implant fibrous tissue models of aseptic implant loosening.

METHODS:

All experiments were approved by the local IACUC.

Mice: All surgeries were performed on 12-16 week-old Lepr-Cre;Tdtomato reporter mice (n=3 for knee arthroplasty model, n=3 for nonunion model, n=3 for POP failure model). In Lepr-Cre;Tdtomato mice, cells of Lepr lineage produce endogenous Tdtomato fluorescent protein (marked red on **Figures 1-3**).

Model of fracture nonunion: Nonunion model was adapted from a reported model (Garcia, P et al. 2007). The femur was exposed through a lateral approach. Osteotomies of 1.8 mm diaphyseal segments were created. A 25-gauge needle with both ends flattened was then inserted into the intramedullary canal through the fracture gap. A clip of 8 mm in length was implanted ventro-dorsally into the femur to provide extra rotational stability and to prevent the collapse of the gap between proximal and distal fragments. The periosteum 2 mm proximal and distal to the gap was stripped along the longitudinal axis.

Model of knee arthroplasty aseptic loosening: We have developed a mouse model using 3D printed titanium (Ti6Al4V) implant to mimic the tibial component of a cementless total knee replacement. The implant is inserted into an over-drilled tibial medullay canal resulting in fibrosis and osseointegration failure.

Model of POP aseptic failure: Circumferential skin incision with posterior skin flap was made approximately 5mm below knee joint. Tibial and peroneal nerves were resected, major vessels were ligated or cauterized. Tibia and fibular shafts were then cut transversely. Muscles from all four compartments were then transected. Intramedullary canal was then retrogradely reamed to 50% larger than the diameter of the implant stem. A titanium implant was then loosely inserted into the canal and the wound was closed by layers.

Confocal imaging: Confocal imaging was conducted.

RESULTS:

At 2 weeks post-surgery, peri-implant lucency was observed in all the mice receiving the over-drilled knee arthroplasty or POP surgery (**Figure 1a & 3a**). Histological analysis of the mice that underwent over-drilled knee arthroplasty and POP both showed the presence of fibrotic tissue in the peri-implant area (**Figures 1b & 3b**). There were abundant flat, elongated, and spindle-shaped cells in the peri-implant area of both models (**Figure 1b (inset) & 3b (inset)**). Confocal imaging of the bone sections showed abundant $LepR^+$ lineage cells in the peri-implant fibrotic tissue (**Figures 1c & 3c**).

At 10 weeks post-surgery, a persistent gap was observed in all the femurs of mice that underwent the fracture nonunion model (**Figure 2a**). Histology showed the presence of fibrotic tissue between the proximal and distal cortices and absent bony bridges between the proximal and distal cortices (**Figures 2b**). There was also abundant flat, elongated, and spindle-shaped cells in the fibrotic tissue (**Figure 2b (inset)**). Confocal imaging of the bone sections showed abundant $LepR^+$ lineage cells in the fibrotic tissue between the proximal and distal cortices (**Figures 2c**).

DISCUSSION AND CONCLUSION:

Our data suggest that LepR marks the fibrotic tissue in fracture nonunion, aseptic loosening, and POP integration failure, thus raising the possibility that $LepR^+$ cells are the common cellular origin for these fibrotic tissues. Further studies to determine the molecular and cellular mechanisms that are broadly activated in the formation of these fibrotic tissues may open a pathway toward pharmaceutical agents to prevent and reverse these unintended fibrotic processes.

SIGNIFICANCE/CLINICAL RELEVANCE: Our finding of involvement of $Lepr^+$ progenitor cells in various orthopaedic pathological fibrous healing is one step closer toward development of pharmaceutical agent to prevent and reverse these pathological fibrotic processes.

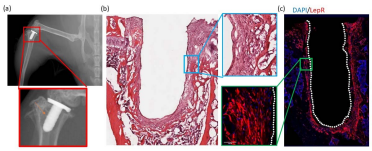

Figure 1: LepR$^+$ lineage cells marks peri-implant fibrosis in knee arthroplasty model. (a) Representative x-ray image of mice underwent overdrilled hemi-knee arthroplasty showing periprosthetic lucency (orange arrow). (b) Representative histology demonstrating the presence of elongated cells in the peri-implant fibrous tissue. (c) Representative confocal imaging of bone sections from LepR-Cre; Tdtomato mice 2-weeks after undergoing the overdrill hemi-arthroplasty model. White dotted-line represents implant-host tissue boundary. Nuclei were visualized using DAPI (blue).

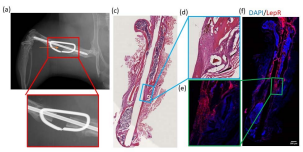

Figure 2: LepR$^+$ lineage cells marks non-union fibrous tissue. (a) Representative x-ray image of mice underwent fracture non-union showing absence of bone in the fracture-gap area after 10 weeks (orange arrow). (b) Representative histology demonstrating the presence of fibrous tissue between the proximal and distal cortex. (c) Representative confocal imaging of bone sections from LepR-Cre; Tdtomato mice 10-weeks after undergoing the fracture non-union model demonstrating abundant presence of LepR$^+$ cells in the fibrotic non-union area. Nuclei were visualized using DAPI (blue).

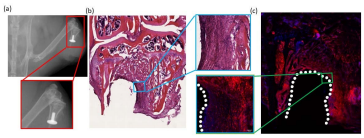

Figure 3: LepR$^+$ lineage cells marks peri-implant fibrotic tissue in percutaneous osseointegrated prosthesis (POP). (a) Representative x-ray image of mice underwent overdrilled percutaneous osseointegrated prosthesis implantation. (b) Representative histology demonstrating the presence of elongated cells in the peri-implant fibrous tissue. (c) Representative confocal imaging of bone sections from LepR-Cre; Tdtomato mice 2-weeks after undergoing the overdrill POP model. White dotted-line represents implant-host tissue boundary. Nuclei were visualized using DAPI (blue).